Probing Topological Entanglement on Large Scales

Robert Ott,[1,2] Torsten V. Zache,[1,2] Nishad Maskara,[3] Mikhail D. Lukin,[3] Peter Zoller,[1,2] and Hannes Pichler[1,2]
[1]Institute for Theoretical Physics, University of Innsbruck, Innsbruck 6020, Austria
[2]Institute for Quantum Optics and Quantum Information of the Austrian Academy of Sciences, Innsbruck 6020, Austria
[3]Department of Physics, Harvard University, Cambridge, Massachusetts 02138, USA

(Received 28 August 2024; revised 5 March 2025; accepted 25 June 2025; published 25 August 2025)

Topologically ordered quantum matter exhibits intriguing long-range patterns of entanglement, which reveal themselves in subsystem entropies. However, measuring such entropies, which can be used to certify topological order, on large partitions is challenging and becomes practically unfeasible for large systems. We propose a protocol based on local adiabatic deformations of the Hamiltonian which extracts the universal features of long-range topological entanglement from measurements on small subsystems of finite size, trading an exponential number of measurements against a polynomial-time evolution. Our protocol is general and readily applicable to various quantum simulation architectures. We apply our method to various string-net models representing both Abelian and non-Abelian topologically ordered phases and illustrate its application to neutral atom tweezer arrays with numerical simulations.

DOI: 10.1103/mdsf-wrbj

Introduction—Long-range quantum correlations play an important role in various areas of physics, ranging from condensed matter [1] to high-energy physics [2] and quantum information science [3]. An example is given by topological order (TO), representing gapped, long-ranged entangled quantum phases, which are robust against local perturbations and characterized by nonlocal order parameters [4,5]. The corresponding ground states feature a long-range structure of entanglement that cannot be undone by local unitary operations [6] and which leads to a universal correction to the area law called the topological entanglement entropy (TEE) S_{topo} [7–9]. Recently, experimental progress for realizations of quantum states with topological entanglement has been enabled by analog quantum simulations with cold neutral atoms [10–12], as well as digital devices based on superconducting qubits [13–16] and trapped ions [17,18].

So far, however, available methods to measure the universal long-range nature of TEE and therefore certify TO, in particular, over large scales, face the experimental challenge of extracting subsystem entropies of large partitions, see Fig. 1. In particular, extracting subsystem entropies without further assumptions on the underlying quantum state [19,20] generically requires a number of measurements that scale exponentially with the partition size [21]; therefore, such entropy measurements are currently restricted to a few qubits [15–18,23]. This prevents direct access to the spatial range of topological

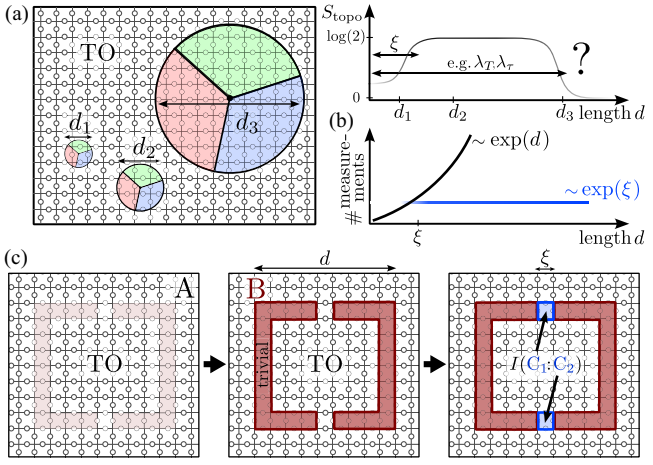


FIG. 1. Protocol. (a) We are interested in the length scale d on which a system exhibits topological entanglement. While TEE can be visible at scales $d \gtrsim \xi$, where ξ is the (short-range) correlation length, it might be absent on large scales $d \gg \xi$, e.g., due to thermal fluctuations (at scale λ_T) [25] or imperfect dynamical preparation (at scale λ_τ) [28,29]. (b) Determining TEE as suggested by Kitaev-Preskill [7] and Levin-Wen [8] at scale d involves measuring entanglement entropies on subsystems of size $\sim d^2$ [see (a)], which generically requires an exponential number of measurements in d. Instead, our protocol requires a fixed number of measurements, set by ξ. (c) We adiabatically deform the system to trivialize region B while A remains TO, including regions C_1, C_2 of size ξ, separated by distance $\sim d$. TEE at scale d is extracted via the mutual information $I(C_1:C_2)$.

Published by the American Physical Society under the terms of the Creative Commons Attribution 4.0 International license. Further distribution of this work must maintain attribution to the author(s) and the published article's title, journal citation, and DOI.

entanglement, which is of crucial interest for probing the stability of TO in large-scale systems [24], see Fig. 1(b).

In this Letter, we overcome this challenge by proposing a novel protocol to efficiently probe TEE in two-dimensional (2D) topological quantum systems. Here, we focus on *robust* TO, which is energetically protected by a Hamiltonian H where both bulk and boundaries of the system are gapped. This includes the doubled topologically ordered phases with parity and time-reversal invariance represented by Levin-Wen string-net models [30]. Our protocol is based on adiabatic local deformations of H that allow us to probe long-range TEE across a large spatial scale d by measuring entropies on regions with finite size of order $\sim\xi$, see Fig. 1, where ξ is the (short-range) correlation length of the medium. More specifically, our protocol removes topologically trivial contributions to the entanglement entropy by decoupling parts of the subsystems indicated as region B in Fig. 1(c), while keeping the universal TEE intact. The decoupling can be achieved in a run-time set by the minimal (finite-size) gap between the TO and a trivial phase in region B, which scales polynomially in its size d if the phases are separated by a second-order transition [31]. We thus effectively trade an exponential (in d) number of measurements for a poly(d)-time evolution followed by $\exp(\xi) \sim \mathcal{O}(1)$ measurements on a reduced partition size. While our protocol is based on coherent many-body evolution and thus requires the associated coherence properties, it is largely robust to microscopic details of the system Hamiltonian. We test the protocol with numerical simulations for a class of experimentally relevant example states and illustrate its application to Rydberg atom arrays, where it can be implemented with current technology.

Protocol—For concreteness, we first focus on the simplest case of $\mathbf{Z}_2$ TO. That is, we consider spins on links of a two-dimensional square lattice (Fig. 1), governed by the toric code (TC) Hamiltonian [3]

$$H_{\mathrm{TC}} = -\epsilon_e \sum_v A_v - \epsilon_m \sum_p B_p. \tag{1}$$

Here $A_v = \prod_{\langle i,v\rangle} Z_i$ represent products of four Pauli-Z operators acting on the links i adjacent to vertices v, and similarly, $B_p = \prod_{i\in\square_p} X_i$ act on the four links within plaquettes p. The magnetic and electric couplings ϵ_m and ϵ_e set the mass scales for excitations of m or e anyons. The ground state $|\psi_{\mathrm{TC}}\rangle$ of H_{TC} is a coherent superposition of all closed-loop states [3]. For simply connected regions R the entanglement entropy $S_R = \mathrm{tr}\rho_R \log(\rho_R)$ of the reduced state ρ_R is

$$S_R = \alpha L_R - S_{\mathrm{topo}}, \tag{2}$$

where L_R is the boundary length of the R, α is a nonuniversal constant, and $S_{\mathrm{topo}} = \log(D)$ is the TEE. D represents the total quantum dimension, which is linked to the nature of TO, and $D = 2$ for the case of $\mathbf{Z}_2$ [7–9]. Directly extracting the value of S_{topo} from Eq. (2) is expensive due to the area law, which dominates S_R at large L_R.

Our protocol to extract S_{topo} instead proceeds as follows: First, we adiabatically introduce an external field $\propto h(t)$, which is localized only in region B (Fig. 1). During this process, the system follows the ground state of $H(t) = H_{\mathrm{TC}} + h(t)\sum_{\ell\in B} Z_\ell$. While the topological structure in the bulk (region A) remains intact, the entanglement structure within both regions B becomes trivial as loops are expelled by the external field as a consequence of e-anyon condensation. They are now forced to pass through the regions C_1 and C_2, where they lead to characteristic correlations that can be detected efficiently [32] via the mutual information [6]

$$I(C_1:C_2) = S_{C_1} + S_{C_2} - S_{C_1C_2}, \tag{3}$$

which, at the end of our protocol, is equal to the topological entropy $I(C_1:C_2) = \log(2)$ [33] (see Supplemental Material [35]). Measuring the subsystem entropies can be achieved using standard techniques, e.g., via tomographic schemes [19] or multicopy measurements [20]. Our protocol allows us to probe TO across the region enclosed by B, i.e., at scale d, while keeping the size of the regions

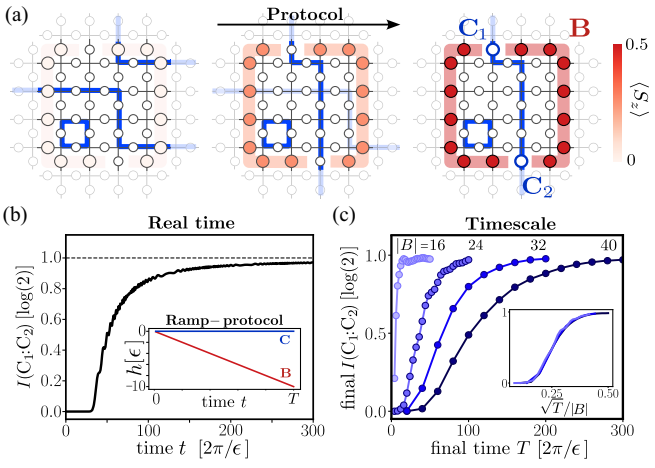


FIG. 2. Protocol illustration for the toric code. (a) The TC ground state can be understood as a superposition of closed loops (left). By turning on a Z field h in region B, the corresponding spins are driven into the state $|\uparrow\rangle$, and the loops are expelled from B and forced to pass through the openings C_1 and C_2 (center and right). This results in a nonzero mutual information $I(C_1:C_2)$ reflecting the long-range patterns of entanglement in TO states of matter. (b) The final value of $I(C_1:C_2)$ yields S_{topo} in the limit of long (adiabatic) ramp times T. (c) The ramp time depends quadratically on the boundary length $|B|$, in accordance with the gap closing of the 1D Ising boundary theory: The curves collapse upon rescaling (inset, for $|B| = 24$, 32, 40).

C_i, and therefore the number of required measurements [see Fig. 1(b)], fixed at the much smaller size ξ^2.

In general, the choice of region B depends on the scale ξ which, for example, results from additional fields in the Hamiltonian. By choosing the regions B to be large and smooth compared to ξ, the long-distance fluctuations are described by effective quantum field theories (QFTs). The protocol drives a transition on the subregion B, between the topological phase described by a Chern-Simons QFT [38] and a topologically trivial phase described by a Higgs QFT. If the transition is of second order (as in the case of $\mathbf{Z}_2$) the gap closes polynomially in the size of region B. Consequently, the protocol can be implemented with a poly(d) run-time. If no second-order transition to a topologically trivial phase exists, our protocol could lead to an exponential run-time that would limit its applicability in large systems.

There are different ways of trivializing the region B, e.g., using longitudinal $[h(t)\sum_{\ell\in B} Z_\ell]$ or transversal $[g(t)\sum_{\ell\in B} X_\ell]$ fields, corresponding to magnetic or electric boundary conditions at the interface with region A. If B is a magnetic boundary, our protocol measures the entropy of electric loops while being insensitive to magnetic loops (and vice versa). This is a consequence of magnetic strings (or m anyons) condensing into B. To probe quantum entanglement and distinguish it from classical topological entropy [25,26], both cases must be probed. Since both cases are dual to each other, we consider the case with longitudinal fields in our numerics below.

Numerical demonstration—In Fig. 2 we numerically demonstrate the protocol for the exact toric code (1). Since the correlation length is $\xi = 0$, B is chosen as a thin, one-dimensional subregion. Ramping up $h(t)$ from zero to $h = 10\epsilon_e = 10\epsilon_m$ at final times T, we drive the spins in region B into their trivial ground state with $\langle S_z\rangle = 1/2$. For a sufficiently slow ramp, we observe the increase of mutual information reaching $I(T) = \log(2)$, while faster, nonadiabatic ramps lead to smaller values. For large systems, the required ramp times T are consistent with a polynomial scaling with the boundary length. This agrees with the linear closing of the gap in the dual Ising theory, i.e., $\Delta \propto N^{-z\nu}$, with critical exponents $z = \nu = 1$ [39].

To go beyond the simple model with $\xi = 0$, we illustrate our idea on a class of states with finite ξ. For this, we consider deformations of $|\psi_{\mathrm{TC}}\rangle$ given by tensor network states which can be efficiently computed for large system sizes [29,40–42],

$$|\psi\rangle \propto e^{\Sigma_\ell (g_\ell^Z Z_\ell + g_\ell^X X_\ell)} |\psi_{\mathrm{TC}}\rangle. \tag{4}$$

The deformation introduces a finite correlation length and leads to a trivial topological structure for $g_Z \gtrsim 0.22$ or $g_X \gtrsim 0.22$ [40]. To confirm that our protocol correctly identifies these phases, we compute the mutual information according to our protocol as shown in Fig. 3(a). For this we mimic

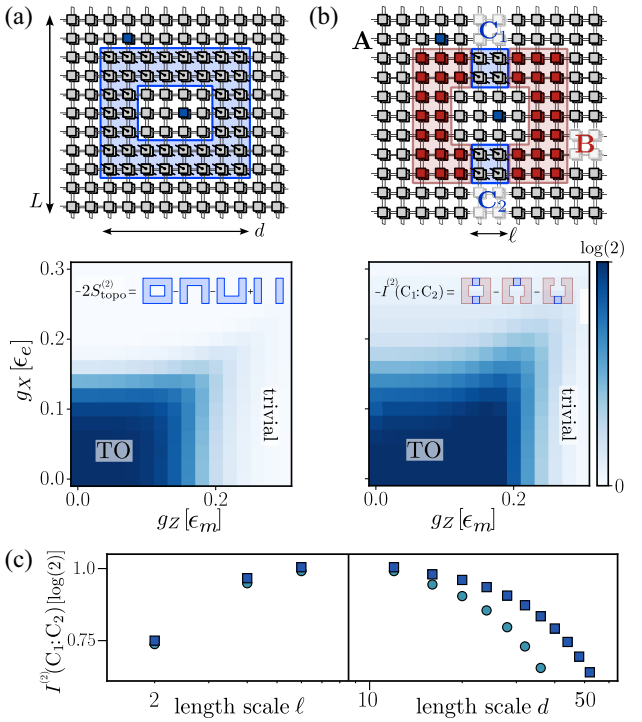


FIG. 3. Detecting the length scale of topological order. (a) We consider 2D tensor network states and extract the topological (Rényi) entropy for various g_X, g_Z. The state phase diagram exhibits a TO and a trivial phase. (b) We locally increase g_B^Z to trivialize the region B (red) and show the mutual information $I^{(2)}(C_1:C_2)$. Shown system sizes $[L,d,\ell]$ are [10,4,2] (a) and [12,4,2] (b). (c) For an incoherent anyon state, the mutual information first increases with ℓ, saturates to log(2) once $\ell \gtrsim \xi$, and decays when d reaches the "thermal" length scale λ_T. Data are shown for $g_Z = 0.15$, $g_X = 0$; e anyons are introduced by locally adapting the tensor structure [blue tensors in (a)] (see Supplemental Material [35] for details).

the final state of a sufficiently slow ramp as (4), where we choose $g_B^Z \gg g_A^Z, g_A^X$ with subscripts A, B indicating the different regions. This allows us to efficiently compute the mutual information of the regions C_1 and C_2 for relatively large spatial scales d, ℓ, and L (Fig. 3). To simplify the computation, we compute second-order Rényi entropies $S^{(2)}_{C_i} = -\log[\mathrm{Tr}(\rho^2_{C_i})]$, rather than von Neumann entropies. This does not change the qualitative features, as the topological Rényi entropy also serves as a topological invariant [43]. Indeed, the result of our construction captures the correct phase boundaries up to finite-size corrections (see Supplemental Material [35]).

Detecting the length scale of topological entropy—We next illustrate the detection of a thermal length scale destroying TO [25] using our protocol. Specifically, consider the mixed state

$$\rho \propto e^{g_Z \Sigma_\ell Z_\ell} e^{-\beta H_{\mathrm{TC}}} e^{g_Z \Sigma_\ell Z_\ell}, \tag{5}$$

corresponding to a thermal toric code state deformed by local fields $\sum_\ell g_Z Z_\ell$. We approximate this state for small temperatures, where the dominant contribution arises from zero- and two-anyon states, as detailed in Supplemental Material [35].

We compute $I^{(2)}(C_1:C_2)$ from the state ρ after trivializing B for different choices of the region B, see Fig. 3(c): We first increase the width ℓ of the regions C_i, while keeping the diameter d of region B fixed. As expected, we obtain log(2), once ℓ surpasses the short-range correlation length, $\ell \gtrsim \xi$. We then keep the scale ℓ fixed and increase the diameter d of region B. Indeed, our protocol detects the disappearance of TEE for distances on the order of the thermal length scale, $d \sim \mathcal{O}(\lambda_T)$.

While we illustrate our protocol for mixed states in this section, it is more general and also applies to pure states. For instance, in the context of adiabatic state preparation with a finite time, we generically expect TO only within finite-sized regions [28,29]. Our protocol would detect topological entanglement for distances d smaller than these regions.

String-net models—As a generalization of the toric code model, we consider different types of TO next. Specifically, we focus on Levin-Wen string-net models [30] based on finite Abelian groups ($\mathbf{Z}_N$) and non-Abelian quantum groups [$\mathrm{SO}(3)_k$], exhibiting the corresponding forms of TO, see Supplemental Material [35].

Following our protocol, we consider the string-net ground state and drive phase transitions to topologically trivial phases in subregions B. In Fig. 4(a) we show the increase of the mutual information during the protocol for the cases $\mathbf{Z}_2$, $\mathbf{Z}_3$, and $\mathbf{Z}_4$, as well as for the analogous protocol for the non-Abelian $\mathrm{SO}(3)_{k=3}$ string-net model hosting Fibonacci anyons. For sufficiently slow execution times, we find the topological contribution $I(C_1:C_2) \to \log(D)$ in the Abelian case with $D = N$, as well as $I(C_1:C_2) \to -\log(D) - 2\sum_{s=0}^{1}(d_s^2/D)\log(d_s/D)$ with $D = d_0^2 + d_1^2$, $d_0 = 1$, and $d_1 = (1+\sqrt{5})/2$ in the non-Abelian, Fibonacci case. The topological values of the mutual information are detailed in Supplemental Material [35].

Application to Rydberg atom arrays—Our ideas are directly applicable to quantum simulators that realize TO phases in their ground states. We illustrate our protocol for Rydberg atom arrays, as recently used to experimentally probe quantum spin liquid states [10]. Specifically, we focus on the PXP model, $H = P[\Omega \sum_i X_i - \Delta \sum_i n_i]P$, with Rabi frequency Ω and detuning Δ. $X_i = |r\rangle_i\langle g|_i + \mathrm{H.c.}$ and $n_i = |r\rangle_i\langle r|_i$ act on the two levels $|g\rangle$ (ground) and $|r\rangle$ (Rydberg) of a single atom i, see Fig. 4(c). The PXP Hamiltonian operates in the fully blockaded subspace (indicated by the blockade projector P), which amounts to neglecting the long-range tails of the Rydberg van der Waals interaction beyond the blockade radius r_b. It serves as a toy model for analog quantum simulation experiments with Rydberg atom arrays [44]. On a ruby lattice, it features a $\mathbf{Z}_2$ TO phase for suitable parameter regimes [45,46].

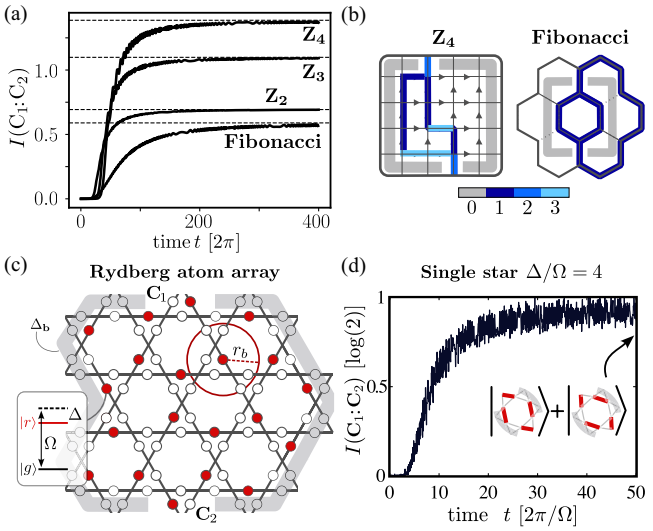


FIG. 4. Generalized protocol. (a) Extraction of TEE with our protocol for Abelian ($\mathbf{Z}_2$, $\mathbf{Z}_3$, $\mathbf{Z}_4$) and non-Abelian (Fibonacci) string-net models (analogous to Fig. 2). (b) Illustration of flux quanta for individual snapshots of the given fixed-point states with the trivialized regions. (c) Proposed implementation with neutral atom tweezer arrays [10]. Local control over detunings Δ of the Rydberg state $|r\rangle$ (see inset) is used to trivialize the boundary (shaded region) by forcing the atoms into their ground states $|g\rangle$. (d) Simulation of the protocol for a small ruby lattice, see Supplemental Material [35] for model parameters. The final state is dominated by the indicated snapshots [with $|\langle \mathrm{inset}|\psi(T)\rangle|^2 \approx 0.58$]. The regions C_1 and C_2 are chosen as the two outermost atoms, respectively.

In Fig. 4(c) we illustrate the protocol for a TO ground state with e boundaries (see also Ref. [45]). TEE is revealed as we ramp the boundary detuning Δ_b of the atoms in the shaded region to force them into their ground states $|g\rangle$, resulting in topological correlations between the regions C_1 and C_2. This process is showcased in Fig. 4(d) for a minimal system (see inset). Over the course of the protocol, the mutual information increases from initially ≈ 0 to the value $\approx \log(2)$ at the final time T. We expect this feature to persist for larger systems with appropriately thickened regions.

Discussion—We have presented a scalable, polynomial-time protocol to measure the topological entanglement structure in 2D quantum systems. This provides a novel tool for probing the stability of TO matter against coherent or incoherent perturbations [25–29]. Our protocol only requires entropies of small subsystems, making it both sample efficient and robust to measurement errors. Importantly, our protocol assumes a Hamiltonian hosting a TO phase and is therefore especially suited for analog quantum simulators. On the one hand, the Hamiltonian preserves the topological structure under the adiabatic deformations of the system; on the other hand, it prevents

the buildup of topological long-range correlations during the protocol if absent initially. However, this also means that our procedure is sensitive to local errors creating pairs of anyons, which could propagate to opposite sides of the trivializing region B and therefore affect the topological structure (see Supplemental Material [35]). While implementing our proposed procedure with high fidelity is, in general, a demanding task, experiments realizing analog adiabatic operations on large systems have been achieved in recent years [47,48].

Our protocol complements other techniques for learning the topological structure of quantum systems, for instance, based on measurements of loop- and string-order parameters [2,49,50]. These nonlocal operators typically decay exponentially with distance, such that it becomes practically unfeasible to determine them on large scales. While this can be mitigated using decorated loop operators [40], our protocol is distinguished by the fact that it is agnostic to such microscopic details.

Generalizations and outlook—Our protocol can be modified in several ways. For instance, instead of adiabatically deforming the Hamiltonian, the topologically ordered states might also directly be prepared in the presence of a trivializing field in region B, e.g., following a generalization of the dynamical preparation protocol studied in Refs. [10,28,29]. Furthermore, a witness for topological, long-range correlations can, in principle, be obtained from measuring correlation functions of only a few local operators between C_1 and C_2, e.g., in only two different bases. This is both sample efficient and avoids the need for complete tomographic control on these regions. Moreover, our protocol could be combined with other novel methods of extracting entropies [22,51–54].

To avoid internal magnetic and electric boundaries, and therefore circumvent the necessity for separate measurements with different boundary conditions, our planar 2D construction can be generalized as shown in Fig. 5. The

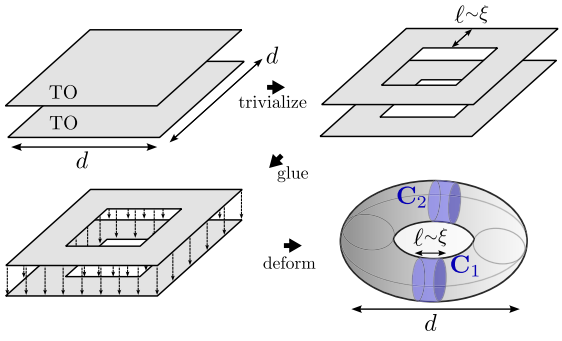


FIG. 5. Gluing a torus. We propose to trivialize, glue, and deform two sheets of topologically ordered matter as shown from left to right. TEE is efficiently extracted through the mutual information between regions C_1 and C_2. This construction avoids physical boundaries in the interior of the sphere (see main text). Spatial features are thickened on the scale of the correlation length ξ.

topological information is contained in the mutual information of two regions C_1 and C_2 [34] and can be measured after gluing two sheets, e.g., by slowly turning on the star and plaquette interactions between the spins at their boundaries. The construction allows us to measure TEE $2\log(2)$ on the scale d with $\mathcal{O}(\exp\xi)$ measurements (Supplemental Material [35]). Combining time-reversed sheets can extend our protocol to chiral topologically ordered phases such as represented by fractional quantum Hall states [7,55], which have recently been realized with neutral atoms in optical potentials [11,12].

Our results are furthermore relevant beyond the 2D Abelian and non-Abelian topologically ordered phases discussed in this Letter. This includes the case of higher dimensions [56] as well as other systems, such as the Yang-Mills gauge theories describing fundamental forces in particle physics [57]. These theories similarly feature nonlocal loop operators, whose long-range entanglement structure could yield further insight into, for instance, the confinement of quarks [2,49].

Acknowledgments—We thank Soonwon Choi, Simon Evered, Alexandra Geim, Byungmin Kang, and Giulia Semeghini for fruitful discussions. N. M. acknowledges support by the Department of Energy Computational Science Graduate Fellowship under Award No. DE-SC0021110. This work is supported by the European Union's Horizon Europe research and innovation program under Grant Agreement No. 101113690 (PASQuanS2.1), the ERC Starting grant QARA (Grant No. 101041435), the EU-QUANTERA project TNiSQ (N-6001), and the Austrian Science Fund (FWF) [Grant DOI. 10.55776/COE1]. Work at Harvard University was supported by IARPA and ARO, under the Entangled Logical Qubits program (Cooperative Agreement No. W911NF-23-2-0219), DARPA ONISQ program (Grant No. W911NF2010021), DARPA IMPAQT program (Grant No. HR0011-23-3-0012), CUA (a NSF Physics Frontiers Center, PHY-1734011), NSF (Grants No. PHY-2012023 and No. CCF-2313084), ARO MURI (Grant No. W911NF-20-1-0082), U.S. Department of Energy [DE-SC0021013 and DOE Quantum Systems Accelerator Center (Contract No. DE-AC02-05CH11231)]. N. M. acknowledges support by the Department of Energy Computational Science Graduate Fellowship under Award No. DE-SC0021110.

Data availability—The data that support the findings of this article are openly available from Zenodo [58].

[1] S. Sachdev, *Quantum Phases of Matter* (Cambridge University Press, Cambridge, England, 2023), 10.1017/9781009212717.
[2] A. M. Polyakov, Nucl. Phys. **B120**, 429 (1977).
[3] A. Y. Kitaev, Ann. Phys. (N.Y.) **303**, 2 (2003).

[4] T. Senthil, A. Vishwanath, L. Balents, S. Sachdev, and M. P. Fisher, Science **303**, 1490 (2004).
[5] J. McGreevy, Annu. Rev. Condens. Matter Phys. **14**, 57 (2023).
[6] B. Zeng, X. Chen, D.-L. Zhou, X.-G. Wen *et al.*, *Quantum Information Meets Quantum Matter* (Springer, New York, 2019), 10.1007/978-1-4939-9084-9.
[7] A. Kitaev and J. Preskill, Phys. Rev. Lett. **96**, 110404 (2006).
[8] M. Levin and X.-G. Wen, Phys. Rev. Lett. **96**, 110405 (2006).
[9] A. Hamma, R. Ionicioiu, and P. Zanardi, Phys. Lett. A **337**, 22 (2005).
[10] G. Semeghini, H. Levine, A. Keesling, S. Ebadi, T. T. Wang, D. Bluvstein, R. Verresen, H. Pichler, M. Kalinowski, R. Samajdar *et al.*, Science **374**, 1242 (2021).
[11] J. Léonard, S. Kim, J. Kwan, P. Segura, F. Grusdt, C. Repellin, N. Goldman, and M. Greiner, Nature (London) **619**, 495 (2023).
[12] P. Lunt, P. Hill, J. Reiter, P. M. Preiss, M. Gałka, and S. Jochim, arXiv:2402.14814.
[13] Z. K. Minev, K. Najafi, S. Majumder, J. Wang, A. Stern, E.-A. Kim, C.-M. Jian, and G. Zhu, Nat. Commun. **16**, 6225 (2025).
[14] Google Quantum AI and Collaborators, Nature (London) **618**, 264 (2023).
[15] K. Satzinger, Y.-J. Liu, A. Smith, C. Knapp, M. Newman, C. Jones, Z. Chen, C. Quintana, X. Mi, A. Dunsworth *et al.*, Science **374**, 1237 (2021).
[16] S. Xu *et al.*, Nat. Phys. **20**, 1469 (2024).
[17] M. Iqbal, N. Tantivasadakarn, R. Verresen, S. L. Campbell, J. M. Dreiling, C. Figgatt, J. P. Gaebler, J. Johansen, M. Mills, S. A. Moses *et al.*, Nature (London) **626**, 505 (2024).
[18] M. Iqbal, N. Tantivasadakarn, T. M. Gatterman, J. A. Gerber, K. Gilmore, D. Gresh, A. Hankin, N. Hewitt, C. V. Horst, M. Matheny *et al.*, Commun. Phys. **7**, 205 (2024).
[19] A. Elben, S. T. Flammia, H.-Y. Huang, R. Kueng, J. Preskill, B. Vermersch, and P. Zoller, Nat. Rev. Phys. **5**, 9 (2023).
[20] A. J. Daley, H. Pichler, J. Schachenmayer, and P. Zoller, Phys. Rev. Lett. **109**, 020505 (2012).
[21] Note that tomography can be made more efficient if assumptions on the quantum state can be made [22].
[22] M. K. Joshi, C. Kokail, R. van Bijnen, F. Kranzl, T. V. Zache, R. Blatt, C. F. Roos, and P. Zoller, Nature (London) **624**, 539 (2023).
[23] A. H. Karamlou, I. T. Rosen, S. E. Muschinske, C. N. Barrett, A. Di Paolo, L. Ding, P. M. Harrington, M. Hays, R. Das, D. K. Kim *et al.*, Nature (London) **629**, 561 (2024).
[24] Mechanisms which can destabilize TO in these systems include thermal fluctuations [25–27] as well as finite coherence or state preparation times [28,29], and they introduce length scales beyond which TO is absent.
[25] C. Castelnovo and C. Chamon, Phys. Rev. B **76**, 184442 (2007).
[26] T.-C. Lu, T. H. Hsieh, and T. Grover, Phys. Rev. Lett. **125**, 116801 (2020).
[27] A. Ritz-Zwilling, J.-N. Fuchs, S. H. Simon, and J. Vidal, Phys. Rev. B **110**, 155147 (2024).
[28] R. Sahay, A. Vishwanath, and R. Verresen, arXiv:2211.01381.
[29] G. Giudici, M. D. Lukin, and H. Pichler, Phys. Rev. Lett. **129**, 090401 (2022).
[30] M. A. Levin and X.-G. Wen, Phys. Rev. B **71**, 045110 (2005).
[31] For gapped boundaries, we can deform the system Hamiltonian without exciting gapless edge modes.
[32] Similarly, as discussed below, one can apply transversal fields to condense m anyons to repel Z loops.
[33] For a TO state, the (long-range) mutual information prior to trivializing the regions is zero for all distant contractible regions, see, e.g., [34].
[34] C.-M. Jian, I. H. Kim, and X.-L. Qi, arXiv:1508.07006.
[35] See Supplemental Material at http://link.aps.org/supplemental/10.1103/mdsf-wrbj for details on the analytical and numerical calculations, which includes Refs. [36,37].
[36] N. E. Bonesteel and D. P. DiVincenzo, Phys. Rev. B **86**, 165113 (2012).
[37] A. Hahn and R. Wolf, Phys. Rev. B **102**, 115154 (2020).
[38] S. Sachdev, Rep. Prog. Phys. **82**, 014001 (2018).
[39] S. Sachdev, Phys. World **12**, 33 (1999).
[40] I. Cong, N. Maskara, M. C. Tran, H. Pichler, G. Semeghini, S. F. Yelin, S. Choi, and M. D. Lukin, Nat. Commun. **15**, 1527 (2024).
[41] J. I. Cirac, D. Perez-Garcia, N. Schuch, and F. Verstraete, Rev. Mod. Phys. **93**, 045003 (2021).
[42] N. Schuch, D. Poilblanc, J. I. Cirac, and D. Pérez-García, Phys. Rev. B **86**, 115108 (2012).
[43] G. B. Halász and A. Hamma, Phys. Rev. A **86**, 062330 (2012).
[44] H. Bernien, S. Schwartz, A. Keesling, H. Levine, A. Omran, H. Pichler, S. Choi, A. S. Zibrov, M. Endres, M. Greiner *et al.*, Nature (London) **551**, 579 (2017).
[45] R. Verresen, M. D. Lukin, and A. Vishwanath, Phys. Rev. X **11**, 031005 (2021).
[46] To stabilize TO in the presence of long-range interactions, the positions of atoms are deformed with respect to the ruby lattice [10,45].
[47] A. Omran, H. Levine, A. Keesling, G. Semeghini, T. T. Wang, S. Ebadi, H. Bernien, A. S. Zibrov, H. Pichler, S. Choi *et al.*, Science **365**, 570 (2019).
[48] P. Scholl, A. L. Shaw, R. B.-S. Tsai, R. Finkelstein, J. Choi, and M. Endres, Nature (London) **622**, 273 (2023).
[49] G. Hooft, Nucl. Phys. **B138**, 1 (1978).
[50] K. Fredenhagen and M. Marcu, Phys. Rev. Lett. **56**, 223 (1986).
[51] B. Vermersch, M. Ljubotina, J. I. Cirac, P. Zoller, M. Serbyn, and L. Piroli, Phys. Rev. X **14**, 031035 (2024).
[52] Y. Teng, R. Samajdar, K. Van Kirk, F. Wilde, S. Sachdev, J. Eisert, R. Sweke, and K. Najaf, arXiv:2406.00193.
[53] T. V. Zache, C. Kokail, B. Sundar, and P. Zoller, Quantum **6**, 702 (2022).
[54] P. Fromholz, G. Magnifico, V. Vitale, T. Mendes-Santos, and M. Dalmonte, Phys. Rev. B **101**, 085136 (2020).
[55] X.-L. Qi, H. Katsura, and A. W. W. Ludwig, Phys. Rev. Lett. **108**, 196402 (2012).
[56] T. Grover, A. M. Turner, and A. Vishwanath, Phys. Rev. B **84**, 195120 (2011).
[57] Đ. Radičević, J. High Energy Phys. 11 (2016) 130.
[58] R. Ott, N. Maskara, T. Zache, M. Lukin, P. Zoller, and H. Pichler, Probing topological entanglement on large scales, Zenodo (2024), 10.5281/zenodo.15910388.